References

1. Kandori A, Miyashita T, Ogata K, Shimizu W, Yokokawa M, Kamakura S, Miyatake K, et al. Magnetocardiography study on ventricular depolarization-current pattern in patients with Brugada syndrome and complete right-bundle branch blocks. Pacing Clinical Electrophysiol 2006; 29:1359–1367.
2. Antzelevitch C, Brugada P, Borggrefe M, Brugada J, Brugada R, Corrado D, Gussak I, et al. Brugada syndrome: Report of the second consensus conference: Endorsed by the Heart Rhythm Society and the European Heart Rhythm Association. Circulation 2005; 111:659–670. Erratum in: Circulation 2005; 112: e74.
3. Shimizu W, Aiba T, Kamakura S. Mechanisms of disease: Current understanding and future challenges in Brugada syndrome. Nat Clin Pract Cardiovasc Med 2005; 2:408–414.
4. Kandori A, Miyashita T, Ogata K, Shimizu W, Yokokawa M, Kamakura S, Miyatake K, et al. Electrical space-time abnormalities of ventricular depolarization in patients with Brugada syndrome and patients with complete right-bundle branch blocks studied by magnetocardiography. Pacing Clinical Electrophysiol 2006; 29:15–20.
5. Kandori A, Shimizu W, Yokokawa M, Noda T, Kamakura S, Miyatake K, Murakami M, et al. Identifying patterns of spatial current dispersion that characterize and separate the Brugada syndrome and complete right-bundle branch block. Med Biol Eng Comput 2004; 42:236–244.

Letter to the Editor

Atrioventricular nodal reentrant tachycardia in the elderly: efficacy and safety of radiofrequency catheter ablation

[Pacing Clin Electrophysiol 2007; 30:S103–S107]

Recently, several groups reported their data on safety and efficacy of catheter ablation of atrioventricular nodal reentrant tachycardia (AVNRT) in the elderly.[1–3] These studies demonstrated that slow pathway ablation for AVNRT is equally safe and effective in older as compared with young patients.

In the January supplement of this journal, Meiltz and Zimmermann[4] published their data on this issue. The authors analyzed a total number of 350 patients who underwent slow-pathway ablation for AVNRT and divided this population into two groups according to age <65 and ≥65 years (280 vs 70 patients). The elderly patient cohort was characterized by an expected age-related alteration of the antegrade atrioventricular (AV) node conduction corroborated by significantly longer atrial-His (AH) and His-ventricular (HV) intervals as well as higher fast pathway effective refractory periods and tachycardia cycle lengths. However, acute ablation success, long-term follow-up, and complication rates were similar in both groups indicating an equal efficacy and safety of catheter ablation in elderly patients suffering from AVNRT. Nevertheless, although particularly older patients are more likely to show contraindications for antiarrhythmic therapy and to develop adverse side effects, catheter ablation should be considered as first line therapy as yet again elegantly underlined in the study by Meiltz and Zimmermann.[4]

However, one aspect deserves a more detailed discussion—the complexity of the ablation procedure in elderly patients. The authors reported[4] that, in contrast to our previous results,[1] they did not observe any differences in procedure durations or fluoroscopy times between both groups and concluded "that RF ablation of AVNRT is not more complex in elderly than in young patients." These controversial findings may result from the diversity of the study populations: our study[1] enrolled 70 patients for the elderly group with an age of ≥75 years with a majority of the patients being octogenarians (mean age 79.4 years), whereas in the study of Meiltz and Zimmermann[4] elderly patients were defined ≥65 years of age (mean age 72 years). Furthermore, our elderly patient cohort was substantially characterized by a preexisting prolonged PR interval. The mean fluoroscopy duration in the younger patient group was markedly shorter in our study as compared to the study of Meiltz and Zimmermann[4] (7.8 min vs 13 min). On the other hand, fluoroscopy durations for the elderly patient group did not demonstrate significant differences in both studies (17.6 min vs 14 min).

In our laboratory, slow pathway ablation in "normal-aged" patients is performed without the use of continuous fluoroscopy during radiofrequency (RF) delivery, particularly when applied at the infero-paraseptal region of the Koch's triangle. This has been established as a safe ablation approach in young patients in our clinical routine. However, in our experience, mapping and ablation conditions are more complex in the elderly due to age-related alterations of cardiac anatomy, i.e. the AV node conduction. In these patients and in patients with a preexisting prolonged PR interval, we use continuous fluoroscopy during RF delivery to avoid minimal changes of the RF catheter position, which may result in inadvertent AV block induction. Thus, slow pathway ablation can be performed safely in elderly patients; however, special caution should be applied when ablating at the slow pathway area in patients with impaired AV conduction to avoid acute AV block induction and to reduce the risk of late high-degree AV-block.[5,6]

In our opinion, even though slow pathway mapping and ablation might be more complex in

LETTERS TO THE EDITOR

Does T_{peak}–T_{end} provide an index of transmural dispersion of repolarization?

To the Editor:

Differences in the time course of repolarization of the three predominant myocardial cell types have been shown to contribute to the inscription of the T wave of the electrocardiogram (ECG). Voltage gradients developing as a result of the different time course of repolarization of phases 2 and 3 in the three cell types give rise to opposing voltage gradients on either side of the M region, which are partly responsible for the inscription of the T wave.[1] In the case of an upright T wave, the epicardial response is the earliest to repolarize, and the M-cell action potential is the latest. In the coronary-perfused wedge preparation, repolarization of the epicardial action potential coincides with the peak of the T wave, and repolarization of the M cells is coincident with the end of the T wave so that the interval from the peak to the end of the T wave provides a measure of transmural dispersion of repolarization (TDR).

Based on these early studies, the T_{peak}–T_{end} interval in precordial ECG leads was suggested to provide an index of TDR.[2] More recent studies also have provided guidelines for estimating TDR in the case of more complex T waves, including negative, biphasic and triphasic T waves.[3] In such cases, the interval from the nadir of the first component of the T wave to the end of the T wave was shown to provide an ECG approximation of TDR.

Although these relationships are relatively straightforward in the coronary-perfused wedge preparation, extrapolation to the surface ECG recorded *in vivo* must be approached with great caution and will require careful validation. The T_{peak}–T_{end} interval is unlikely to provide an absolute measure of transmural dispersion *in vivo*, as elegantly demonstrated by Xia et al.[4] However, changes in this parameter are thought to be capable of reflecting changes in spatial dispersion of repolarization, particularly TDR, and thus may be prognostic of arrhythmic risk under a variety of conditions.[5–10] Takenaka et al[9] demonstrated exercise-induced accentuation of the T_{peak}–T_{end} interval in patients with long QT syndrome (LQTS) type 1 (LQT1) but not LQT2. These observations, coupled with those of Schwartz et al[11] demonstrating an association between exercise and risk for torsades de pointes in patients with LQT1 but not LQT2, point to the potential value of T_{peak}–T_{end} in forecasting the risk for development of torsades de pointes. Direct evidence supporting T_{peak}–T_{end} as an index for predicting torsades de pointes in patients with LQTS was provided by Yamaguchi et al.[12] These authors concluded that T_{peak}–T_{end} is more valuable than QTc and QT dispersion as a predictor of torsades de pointes in patients with acquired LQTS. Shimizu et al[8] demonstrated that T_{peak}–T_{end}, but not QTc, predicted sudden cardiac death in patients with hypertrophic cardiomyopathy. In a case control study comparing 30 cases of acquired bradyarrhythmias complicated by torsades de pointes and 113 cases with uncomplicated bradyarrhythmias, Topilski et al[13] found that QT, QTc, and T_{peak}–T_{end} intervals were strong predictors of torsades de pointes, with prolonged T_{peak}–T_{end} as the best single discriminator. Watanabe et al[10] demonstrated that prolonged T_{peak}–T_{end} is associated with inducibility as well as spontaneous development of ventricular tachycardia in high-risk patients with organic heart disease.

These interesting studies demonstrating an association between an increase in T_{peak}–T_{end} and arrhythmic risk notwithstanding, direct validation of T_{peak}–T_{end} measured at the body surface as an index of TDR is still lacking. Guidelines for such validation have been suggested repeatedly.[1,3,14] Because the precordial leads view the electrical field across the ventricular wall, T_{peak}–T_{end} would be expected to be most representative of TDR in these leads. The precordial leads are unipolar leads placed on the chest that are referenced to Wilson central terminal. The direction of these leads is radially outward from the "center" of the heart, the center of the Einthoven triangle. Unlike the precordial leads, the bipolar limb leads, including leads I, II, and III, do not look across the ventricular wall. Although T_{peak}–T_{end} intervals measured in these limb leads may provide an index of TDR, they are more likely to reflect global dispersion, including apicobasal and interventricular dispersion of repolarization.[4,15]

A large increase in TDR is likely to be arrhythmogenic because the dispersion of repolarization and refractoriness occurs over a very short distance (the width of the ventricular wall), creating a steep repolarization gradient.[16,17] It is the steepness of the repolarization gradient rather than the total magnitude of dispersion that determines its arrhythmogenic potential. Apicobasal or interventricular dispersion of repolarization is less informative because it may or may not be associated with a steep repolarization gradient and thus may or may not be associated with arrhythmic risk.

The other critical point to consider is that TDR can be highly variable in different regions of the ventricular myocardium, particularly under pathophysiologic conditions. Consequently, it is important to measure T_{peak}–T_{end} independently in each of the precordial leads, and it is inadvisable to average T_{peak}–T_{end} among several leads.[4] Because LQTS is principally a left ventricular disorder, TDR is likely to be greatest in the left ventricular wall or septum and thus to be best reflected in left precordial leads or V_3, respectively. In their study of acquired LQTS, Yamaguchi

et al[12] targeted lead V_5. In contrast, because Brugada syndrome is a right ventricular disorder, TDR is greatest in the right ventricular free wall and thus is best reflected in the right precordial leads. For this reason, Castro et al[18] targeted lead V_2 in their study. Therefore, the criteria for validation of T_{peak}–T_{end} as an index of TDR are fairly simple, requiring that (1) individual precordial leads, and not bipolar limb leads, be evaluated and (2) TDR be present at baseline and significantly augmented as a result of an intervention.

In the March 2007 issue of *Heart Rhythm*, Opthof et al[15] set out to test the hypothesis T_{peak}–T_{end} interval reflects transmural dispersion. Plunge electrodes were used to quantitate transmural and global dispersion of repolarization, and T_{peak}–T_{end} (T_{p-e}) was measured only in a single limb lead, lead II, under conditions in which TDR was essentially nonexistent: 2.7–14.5 ms. The use of two anesthetics, propofol and isoflurane, known to suppress sodium channel currents in a variety of cells, including M cells, together with the use of a pacing rate of 130 bpm, resulted in essentially no TDR. The recording of precordial ECGs was not possible in this open chest dog model. Thus, the two fundamental criteria for validation were not met, and the study as designed, for reasons discussed above, could come to no other conclusion than that reached, which is that "T_{p-e} does not correlate with transmural dispersion of repolarization but is an index of total dispersion of repolarization."

Thus, the quest for direct validation or invalidation of T_{peak}–T_{end} measured at the body surface as an index of TDR remains unfulfilled. Although most studies to date concur that T_{peak}–T_{end} provides a measure of spatial dispersion of repolarization, the extent to which an augmented T_{peak}–T_{end} interval is prognostic of arrhythmic risk depends on the proximity of the regions displaying disparate repolarization times (i.e., repolarization gradient). Consequently, it would be helpful to know to what extent T_{peak}–T_{end} provides an index of TDR, in which case the differences in refractoriness are ensured to be within close proximity. To this end, it is noteworthy that an ideal model in which to test the hypothesis is the chronic atrioventricular (AV) block dog treated with I_{Kr} blockers, because changes in T_{peak}–T_{end} could be accurately correlated with TDR in a model that displays prominent TDR and additionally correlated with the risk for development of torsades de pointes.

Charles Antzelevitch, PhD, FHRS
ca@mmrl.edu
Serge Sicouri, MD
José M. Di Diego, MD
Alexander Burashnikov, PhD

Masonic Medical Research Laboratory
Utica, New York

Sami Viskin, MD

Department of Cardiology
Tel-Aviv Sourasky Medical Center, and
Sackler School of Medicine, Tel-Aviv University
Tel Aviv, Israel

Wataru Shimizu, MD, PhD

Division of Cardiology, Department of Internal Medicine
National Cardiovascular Center
Suita, Osaka, Japan

Gan-Xin Yan, MD, PhD
Peter Kowey, MD

Main Line Health Heart Center
Wynnewood, Pennsylvania, and
Jefferson Medical College of Thomas Jefferson University
Philadelphia, Pennsylvania

Li Zhang, MD

Department of Cardiology
LDS Hospital, Intermountain Healthcare
University of Utah School of Medicine
Salt Lake City, Utah

References

1. Yan GX, Antzelevitch C. Cellular basis for the normal T wave and the electrocardiographic manifestations of the long QT syndrome. Circulation 1998;98:1928–1936.
2. Antzelevitch C, Shimizu W, Yan GX, Sicouri S, Weissenburger J, Nesterenko VV, Burashnikov A, Di Diego JM, Saffitz J, Thomas GP. The M cell: its contribution to the ECG and to normal and abnormal electrical function of the heart. J Cardiovasc Electrophysiol 1999;10:1124–52.
3. Emori T, Antzelevitch C. Cellular basis for complex T waves and arrhythmic activity following combined I(Kr) and I(Ks) block. J Cardiovasc Electrophysiol 2001;12:1369–1378.
4. Xia Y, Liang Y, Kongstad O, Liao Q, Holm M, Olsson B, Yuan S. In vivo validation of the coincidence of the peak and end of the T wave with full repolarization of the epicardium and endocardium in swine. Heart Rhythm 2005;2:162–169.
5. Wolk R, Stec S, Kulakowski P. Extrasystolic beats affect transmural electrical dispersion during programmed electrical stimulation. Eur J Clinical Invest 2001;31:293–301.
6. Tanabe Y, Inagaki M, Kurita T, Nagaya N, Taguchi A, Suyama K, Aihara N, Kamakura S, Sunagawa K, Nakamura K, Ohe T, Towbin JA, Priori SG, Shimizu W. Sympathetic stimulation produces a greater increase in both transmural and spatial dispersion of repolarization in LQT1 than LQT2 forms of congenital long QT syndrome. J Am Coll Cardiol 2001;37:911–919.
7. Frederiks J, Swenne CA, Kors JA, van Herpen G, Maan AC, Levert JV, Schalij MJ, Bruschke AV. Within-subject electrocardiographic differences at equal heart rates: role of the autonomic nervous system. Pflugers Arch 2001;441:717–724.
8. Shimizu M, Ino H, Okeie K, Yamaguchi M, Nagata M, Hayashi K, Itoh H, Iwaki T, Oe K, Konno T, Mabuchi H. T-peak to T-end interval may be a better predictor of high-risk patients with hypertrophic cardiomyopathy associated with a cardiac troponin I mutation than QT dispersion. Clin Cardiol 2002;25:335–339.
9. Takenaka K, Ai T, Shimizu W, Kobori A, Ninomiya T, Otani H, Kubota T, Takaki H, Kamakura S, Horie M. Exercise stress test amplifies genotype-phenotype correlation in the LQT1 and LQT2 forms of the long-QT syndrome. Circulation 2003;107:838–844.
10. Watanabe N, Kobayashi Y, Tanno K, Miyoshi F, Asano T, Kawamura M, Mikami Y, Adachi T, Ryu S, Miyata A, Katagiri T. Transmural dispersion of repolarization and ventricular tachyarrhythmias. J Electrocardiol 2004;37:191–200.
11. Schwartz PJ, Priori SG, Spazzolini C, Moss AJ, Vincent GM, Napolitano C, Denjoy I, Guicheney P, Breithardt G, Keating MT, Towbin JA, Beggs AH, Brink P, Wilde AA, Toivonen L, Zareba W, Robinson JL, Timothy KW, Corfield V, Wattanasirichaigoon D, Corbett C, Haverkamp W, Schulze-Bahr E, Lehmann MH, Schwartz K, Coumel P, Bloise R. Genotype-phenotype correlation in the long-QT syndrome: gene-specific triggers for life-threatening arrhythmias. Circulation 2001;103:89–95.
12. Yamaguchi M, Shimizu M, Ino H, Terai H, Uchiyama K, Oe K, Mabuchi T, Konno T, Kaneda T, Mabuchi H. T wave peak-to-end interval and QT dispersion in acquired long QT syndrome: a new index for arrhythmogenicity. Clin Sci (Lond) 2003;105:671–676.
13. Topilski I, Rogowski O, Rosso R, Justo D, Copperman Y, Glikson M, Belhassen B, Hochenberg M, Viskin S. The morphology of the QT interval predicts torsade de pointes during acquired bradyarrhythmias. J Am Coll Cardiol 2007;49:320–328.

14. Antzelevitch C. T peak-Tend interval as an index of transmural dispersion of repolarization. Eur J Clin Invest 2001;31:555–557.
15. Opthof T, Coronel R, Wilms-Schopman FJG, Plotnikov AN, Shlapakova IN, Danilo P Jr, Rosen MR, Janse MJ. Dispersion of repolarization in canine ventricle and the electrocardiographic T wave: T_{p-e} interval does *not* reflect transmural dispersion. Heart Rhythm 2007;4:341–348.
16. Akar FG, Yan GX, Antzelevitch C, Rosenbaum DS. Unique topographical distribution of M cells underlies reentrant mechanism of torsade de pointes in the long-QT syndrome. Circulation 2002;105:1247–1253.
17. Aiba T, Shimizu W, Hidaka I, Uemura K, Noda T, Zheng C, Kamiya A, Inagaki M, Sugimachi M, Sunagawa K. Cellular basis for trigger and maintenance of ventricular fibrillation in the Brugada syndrome model: high-resolution optical mapping study. J Am Coll Cardiol 2006;47:2074–2085.
18. Castro HJ, Antzelevitch C, Tornes BF, Dorantes SM, Dorticos BF, Zayas MR, Quinones Perez MA, Fayad RY. Tpeak-Tend and Tpeak-Tend dispersion as risk factors for ventricular tachycardia/ventricular fibrillation in patients with the Brugada syndrome. J Am Coll Cardiol 2006;47:1828–1834.

A wedge is not a heart

To the Editor—Response:

We recently reported that the interval between the peak (T_{peak}) and the end (T_{end}) of the T wave (T_{p-e}) in lead II of the ECGs of *in situ* canine hearts is neither the equivalent nor an index of transmural dispersion of repolarization.[1] We did not query the importance of the T_{p-e} interval but only the mechanism responsible for it. Our finding was in contrast to that in ventricular wedge preparations obtained from the free wall of the canine left ventricle in which Antzelevitch et al[2] not only have reported that the T_{p-e} interval of a surrogate ECG reflects transmural dispersion of repolarization but have argued that this finding applies to the *in situ* heart as well. The difference between the significance of the T_{p-e} interval in an *in situ* heart and in a preparation derived from it is discussed in the letter from Antzelevitch et al, who raise several issues to which we will respond.

The nature of the argument

If we are to argue whether the heart manifests an outcome (the T_{p-e} interval) as the result of one specific gradient, then the evidence considered must permit us to weigh this gradient against all other possible gradients, be they transmural, apicobasal, anteroposterior, or even global. Yet while the intact heart has the property to manifest all such gradients, the wedge preparation shows only one. How then can the wedge be used to conclude that gradients other than the transmural do not contribute to the T_{p-e} interval? And if one wishes to understand the physiology of the *in situ* heart, are not data from lead II in an ECG of an *in situ* heart at least as relevant as data from a bipolar electrogram (a surrogate ECG) of a wedge preparation recorded in a tissue bath?

The wedge preparation and the *in vivo* heart

The letter by Antzelevitch et al reiterates that the long time-course of M-cell repolarization in a ventricular wedge preparation is relevant for the configuration of the T wave in an artificial ECG. By translating the observations in the wedge preparation (earliest repolarization occurring in the epicardium, concurrent with the peak of the T wave; latest repolarization in an M-cell layer, concurrent with the end of the T wave; and endocardial repolarization interposed between the others), the authors implicitly assume that there is no significant dispersion along the endocardium and along the epicardium. The right panel of Figure 2 of our article[1] demonstrates that such dispersion occurs and is of the same order as total dispersion in the *in situ* heart.

The wedge provides a reductionist model, and we believe that reductionism should aim at facilitating our understanding of normal and abnormal function of the intact organ. However, when the wedge becomes the surrogate of the heart and its surrogate ECG is substituted for the body surface ECG, the seductive simplicity of resultant explanations and interpretations can serve to confuse scientist and clinician alike. To understand this comment, one need only reflect that the T wave of the surrogate ECG of the wedge is concordant with the QRS complex, whereas in most ECG leads in the intact dog the T wave is discordant with the QRS complex.[3–5]

There are also methodologic problems with the wedge. First, myocytes may uncouple from each other at the cut surface of the preparation where action potentials are recorded. At the very least, they lack the electrotonic influence of the remainder of the ventricle (not included in the wedge) even when the preparation has healed over. Action potentials, in general, are shorter in the *intact* heart than in single myocytes or pieces of tissue or the wedge preparation.[6,7] In addition, a review of the literature finds no evidence for late repolarization in the midmyocardium in the *in situ* heart.[7,8]

Finally, it is important to note that even when these limitations of the wedge are understood, Zipes' group[9] was unable to confirm the existence of a midmural zenith in action potential duration, notably at an unphysiologically long cycle length, a condition known to favor the unmasking of the long action potentials of M cells.

The meaning of an increased T_{p-e} interval

Antzelevitch et al argue that increased T_{p-e} intervals are associated with an increased propensity to arrhythmias in several cardiac diseases. Our article[1] does not state that an increased T_{p-e} interval is not a useful parameter. This is not at debate. Rather, what is at debate is what underlies the T_{p-e} interval. Although this may be transmural dispersion of repolarization in the wedge preparation, in the *in situ* heart it is far better explained by total dispersion of repolarization.[1,10,11]

Dispersion and distance

Antzelevitch et al state that "*A large increase in TDR* [transmural dispersion of repolarization] *is likely to be arrhythmogenic because the dispersion of repolarization and refractoriness occurs over a very short distance (the width of the ventricular wall), creating a steep repolar-*

Comparison of Long-Term Follow-Up of Electrocardiographic Features in Brugada Syndrome Between the SCN5A-Positive Probands and the SCN5A-Negative Probands

Miki Yokokawa, MD, Takashi Noda, MD, PhD, Hideo Okamura, MD, Kazuhiro Satomi, MD, PhD, Kazuhiro Suyama, MD, PhD, Takashi Kurita, MD, PhD, Naohiko Aihara, MD, Shiro Kamakura, MD, PhD, and Wataru Shimizu, MD, PhD*

To investigate changes of electrocardiographic parameters with aging and their relation to the presence of SCN5A mutation in probands with Brugada syndrome (BS), we measured several electrocardiographic parameters prospectively during long-term follow-up (10 ± 5 years) in 8 BS probands with SCN5A mutation (SCN5A-positive group, all men; age 46 ± 10 years) and 36 BS probands without SCN5A mutation (SCN5A-negative group, all men; age 46 ± 13 years). Throughout the follow-up period, depolarization parameters, such as P-wave (lead II), QRS (leads II, V_2, V_5), S-wave durations (leads II, V_5), and PQ interval (leads II) were all significantly longer and S-wave amplitude (II, V_5) was significantly deeper in the SCN5A-positive group than in the SCN5A-negative group. The SCN5A-positive group showed a significantly longer corrected QT interval (lead V_2) and higher ST amplitude (lead V_2) than those in the SCN5A-negative group. The depolarization parameters increased with aging during the follow-up period in both groups; however, the PQ interval (lead II) and QRS duration (lead V_2) were prolonged more prominently and the QRS axis deviated more to the left with aging in the SCN5A-positive group than in the SCN5A-negative group. In conclusion, conduction slowing was more marked and more progressively accentuated in Brugada probands with SCN5A mutation than in those without SCN5A mutation. **(Am J Cardiol 2007; 100:649–655)**

Brugada syndrome (BS) is characterized by a ST-segment elevation in the right precordial leads V_1 to V_3 and is associated with sudden cardiac death (SCD) secondary to a rapid polymorphic ventricular tachycardia (VT) or ventricular fibrillation (VF).[1–9] It has been suggested that a transient outward current-mediated action potential notch and a loss of action potential dome in the epicardium of the right ventricular outflow tract (RVOT) give rise to a transmural voltage gradient, resulting in ST-segment elevation in the right precordial lead in BS.[8] Conversely, the SCN5A gene encoding the cardiac sodium channel has been reported to be linked to BS,[10] and mild conduction abnormalities and QRS prolongation have been described.[5,11] Smits et al[12] have compared these electrocardiographic parameters between SCN5A mutation carriers and those who do not carry the mutation. Probst et al[13] meticulously studied aging-associated electrocardiographic parameters in SCN5A-related BS.[13] However, progressive changes of the depolarization and repolarization parameters on the electrocardiogram (ECG) with aging during long-term follow-up in relation to the SCN5A mutation have not been fully evaluated. In the present study, we prospectively measured several electrocardiographic parameters during long-term follow-up periods and compared them between patients with BS with and without SCN5A mutation.

Methods

The study population consisted of 44 probands with BS admitted to the National Cardiovascular Center in Suita, Japan, due to history of aborted SCD, syncope, or evaluation of electrocardiographic abnormality, who could be prospectively followed up for >5 years (average 10 ± 5 years) at regular outpatient clinics in our hospital. All probands were men, and their age on admission (i.e., at early period) ranged from 20 to 72 years (mean 46 ± 12 years). BS was diagnosed when a type 1 coved-type ST-segment elevation (≥0.2 mV at J point) was observed in >1 of the right precordial leads (V_1 to V_3) in the presence or absence of a sodium channel blocker in conjunction with 1 of the following: (1) documented VF or polymorphic VT, (2) a family history of SCD at <45 years of age, type 1 ECG in family members, (3) inducibility of VF or polymorphic VT with programmed electrical stimulation, and (4) history of aborted cardiac arrest with or without documentation of VF,

Division of Cardiology, Department of Internal Medicine, National Cardiovascular Center, Suita, Osaka, Japan. Manuscript received February 6, 2007; revised manuscript received and accepted March 15, 2007.

Dr. Shimizu was supported by the Uehara Memorial Foundation, Tokyo; the Hoansha Research Foundation, Osaka; Japan Research Foundation for Clinical Pharmacology, Tokyo; Ministry of Education, Culture, Sports, Science and Technology Leading Project for Biosimulation, Tokyo; and health sciences research grants (H18-Research on Human Genome-002) from the Ministry of Health, Labor and Welfare, Tokyo, Japan.

*Corresponding author: Tel: 81-6-6833-5012; fax: 81-6-6872-7486.
E-mail address: wshimizu@hsp.ncvc.go.jp (W. Shimizu).

0002-9149/07/$ – see front matter
doi:10.1016/j.amjcard.2007.03.078

Table 1
SCN5A mutations, common variants and promotor haplotype

Coding*	No. of Patients	Type	Coding	No. of Patients	Type
	SCN5A Positive Group (n = 8)			SCN5A Negative Group (n = 36)	
Mutation					
A735V	1	Missense			
P1719fsX1786	1	Frameshift			
L276Q	1	Missense			
V1764fsX1786	1	Frameshift			
L136P	1	Missense			
R367H	2	Missense			
T1709M	1	Missense			
Common variant					
H558R	1	Missense	H558R	4	Missense
Promotor haplotype					
AA	5		AA	12	
AB	2		AB	4	
BB	0		BB	1	

* The numbers and letters refer to the amino acid coding of the mutant channel protein.
AA = haplotype A (common alleles) homozygotes; AB = haplotype A/haplotype B (minor alleles) heterozygotes; BB = haplotype B homozygotes. See detail in Bezzina et al.[14]

syncopal episodes of unknown origin, or nocturnal agonal respiration.[4]

We divided the 44 Brugada probands into 2 groups according to the presence or absence of an SCN5A coding region mutation: SCN5A-positive group (n = 8) and SCN5A-negative group (n = 36).

The standard 12-lead ECGs were recorded at least every 6 months prospectively at regular outpatient clinics with a paper speed of 25 mm/s and an amplitude of 10 mm/mV. The ECGs were magnified to 150%, and several electrocardiographic parameters were measured manually by an investigator (MY) blinded to clinical and genetic information. As depolarization parameters, P-wave duration (lead II), PQ interval (lead II), QRS duration (leads II, V_2, and V_5), S-wave duration and amplitude (leads II, V_5), and QRS axis were measured. Conversely, corrected QT interval (QTc, leads II, V_2, and V_5), corrected JT interval (JTc, leads II, V_2, and V_5), and ST amplitude at the J point and 40 ms after theJ point (STJ and STJ40, lead V_2) were measured as repolarization parameters. The absolute values of these parameters and the change of each parameter between early and late periods were compared between the 8 probands in the SCN5A-positive group and the 36 in the SCN5A-negative group.

In all patients, we screened SCN5A mutation in all 28 exons of SCN5A gene by a direct sequencing method using an ABI 3700 system (Applied Biosystems, Foster City, California). An SCN5A mutation was defined when the mutation was not identified in any of the 100 control subjects. We also screened the SCN5A promoter haplotype, which we have recently identified in an Asian population,[14] in 7 recent SCN5A-positive probands and 17 SCN5A-negative probands.

Numeric values were expressed as means ± SD. Comparisons of each electrocardiographic parameter between the SCN5A-positive group and the SCN5A-negative group and between the early and the late periods were made using 2-way repeated-measures analysis of variance (ANOVA) followed by the Scheffe multiple-comparison test. Comparisons of changes in each parameter between the SCN5A-positive group and the SCN5A-negative group were made using 1-way ANOVA followed by Scheffe test. Comparisons of the clinical, electrophysiologic, and follow-up data between the SCN5A-positive group and the SCN5A-negative group were made using chi-square test or 1-way ANOVA followed by Scheffe test. A p value <0.05 was considered significant.

Results

The SCN5A mutations, which were identified at a coding region in the SCN5A-positive group, are shown in Table 1. Five missense mutations and 2 frameshift mutations were identified. A missense mutation, R367H, was identified in 2 unrelated Brugada probands. The common variant and SCN5A promoter haplotype[14] in both groups are also shown in Table 1. There were no significant differences in the frequency of the common variant and the promoter haplotype between the 2 groups.

The comparison of the clinical and electrophysiologic characteristics between the 8 SCN5A-positive probands and the 36 SCN5A-negative probands are shown in Table 2. There were no significant differences in the age on admission, when the clinical diagnosis of BS was made, between the 2 groups. No significant differences were observed in the incidence of spontaneous type 1 ECG, documented VF until the early period, family history of SCD, implantation of implantable cardioverter defibrillator, complete right bundle branch block (RBBB) at the early period and the latest follow-up period (i.e., late period), and late potentials. The HV interval during the electrophysiologic study was significantly longer in the SCN5A-positive group than in the SCN5A-negative group. There were no significant differ-

Table 2
Clinical and electrophysiologic characteristics and follow-up

Characteristic	SCN5A-Positive Group (n = 8)	SCN5A-Negative Group (n = 36)	p Value
Clinical characteristics			
Age on admission (yrs)	46 ± 10	46 ± 13	0.938
Spontaneous type 1 ECG	6 (75%)	25 (69%)	0.755
Documented VF until early period	2 (25%)	17 (47%)	0.251
Family history of SCD	3 (38%)	4 (11%)	0.065
ICD implantation	8 (100%)	26 (72%)	0.090
Complete RBBB at early period	1 (13%)	2 (5%)	0.481
Complete RBBB at late period	1 (13%)	6 (17%)	0.771
Late potentials	7/7 (100%)	24/33 (73%)	0.117
Electrophysiologic characteristics			
Induction of VF	5/8 (63%)	25/33 (76%)	0.658
Mode (triple/double/single)	1/3/1	12/11/2	-
HV interval (ms)	65±5 (n=7)	41±8 (n=27)	<0.001
Follow-up			
Follow-up period (yrs)	10 ± 5	10 ± 4	0.993
Arrhythmic events during follow-up periods	4/8 (50%)	12/36 (33%)	0.375
Previous VF	2/2 (100%)	8/17 (47%)	0.156
No previous VF	2/6 (33%)	4/19 (21%)	0.539

EPS = electrophysiological study; HV = His-ventricular interval; ICD = implantable cardioverter-defibrillator.

ences in the frequency and mode of VF induction between the 2 groups.

Figure 1 illustrates the standard 12-lead ECGs at early and late periods during the follow-up period in representative patients with BS in the SCN5A-positive group (Figure 1) and the SCN5A-negative group. Table 3 shows composite data of the electrocardiographic parameters at the early and late periods in the 8 SCN5A-positive probands and 36 SCN5A-negative probands during the follow-up period.

As depolarization parameters, the P-wave duration (lead II), PQ interval (lead II), and QRS duration (lead II) significantly increased with aging from early to late periods in both groups and were all significantly longer in the SCN5A-positive group than in the SCN5A-negative group at both early and late periods. The QRS duration (lead V_2) in the SCN5A-positive group and the S-wave duration (leads II and V_5) in the SCN5A-negative group significantly increased with aging. The QRS duration (leads V_2 and V_5) and the S-wave duration (leads II and V_5) were significantly longer, and the S-wave amplitude (leads II and V_5) was significantly deeper in the SCN5A-positive group at early and late periods. The QRS axis was not different between the 2 groups at the early period; however, it was significantly smaller (i.e., deviated to the left) at the late period in the SCN5A-positive group.

As a repolarization parameter, the corrected QT interval (lead V_2) was significantly prolonged from the early period to the late period in the SCN5A-positive group, and was significantly longer in the SCN5A-positive group than in the SCN5A-negative group at the early and late periods. However, the QTc intervals (leads II and V_5) did not change from the early period to the late period in both groups and were not different between groups at the early and late periods. Conversely, no JTc intervals (leads II, V_2, and V_5) changed from the early period to the late period in both groups, and the JTc interval (lead V_2) at the late period was significantly longer in the SCN5A-positive group. The STJ amplitude (lead V_2) and STJ40 amplitude (lead V_2) did not change throughout the follow-up period in both groups, but were significantly greater in the SCN5A-positive group than in the SCN5A-negative group at the early and late periods. Even if we eliminated probands with BS with complete RBBB (1 SCN5A-positive proband and 2 SCN5A-negative probands at the early period, 1 SCN5A-positive proband and 6 SCN5A-negative probands at the late period), the main results and statistical differences were not significant.

Table 4 depicts comparison of the change of the electrocardiographic parameters from early to late periods between the SCN5A-positive group and the SCN5A-negative group.

The changes in PQ interval (lead II) and QRS duration (lead V_2) were significantly longer in the SCN5A-positive group than in the SCN5A-negative group. The change in QRS axis was greater (i.e., deviated more to the left) in the SCN5A-positive group than in the SCN5A-negative group.

There were no significant differences in the duration of follow-up period and the incidence of arrhythmic events during the follow-up period between the 2 groups (Table 2). Because a history of documented VF (until the early period) was proven to be the strongest predictor for subsequent arrhythmic events, arrhythmic events were compared between the 2 groups separately in probands with previous VF and those without previous VF, but no significant differences were observed (Table 2).

Discussion

The present study includes what is, to our knowledge, the longest follow-up of changes of electrocardiographic parameters in SCN5A-positive probands and SCN5A-negative probands with BS.

Mild conduction abnormalities, such as widening of the P wave, prolongation of QRS duration and PQ and HV intervals, and higher incidence of RBBB, have been described in patients with BS, especially those with

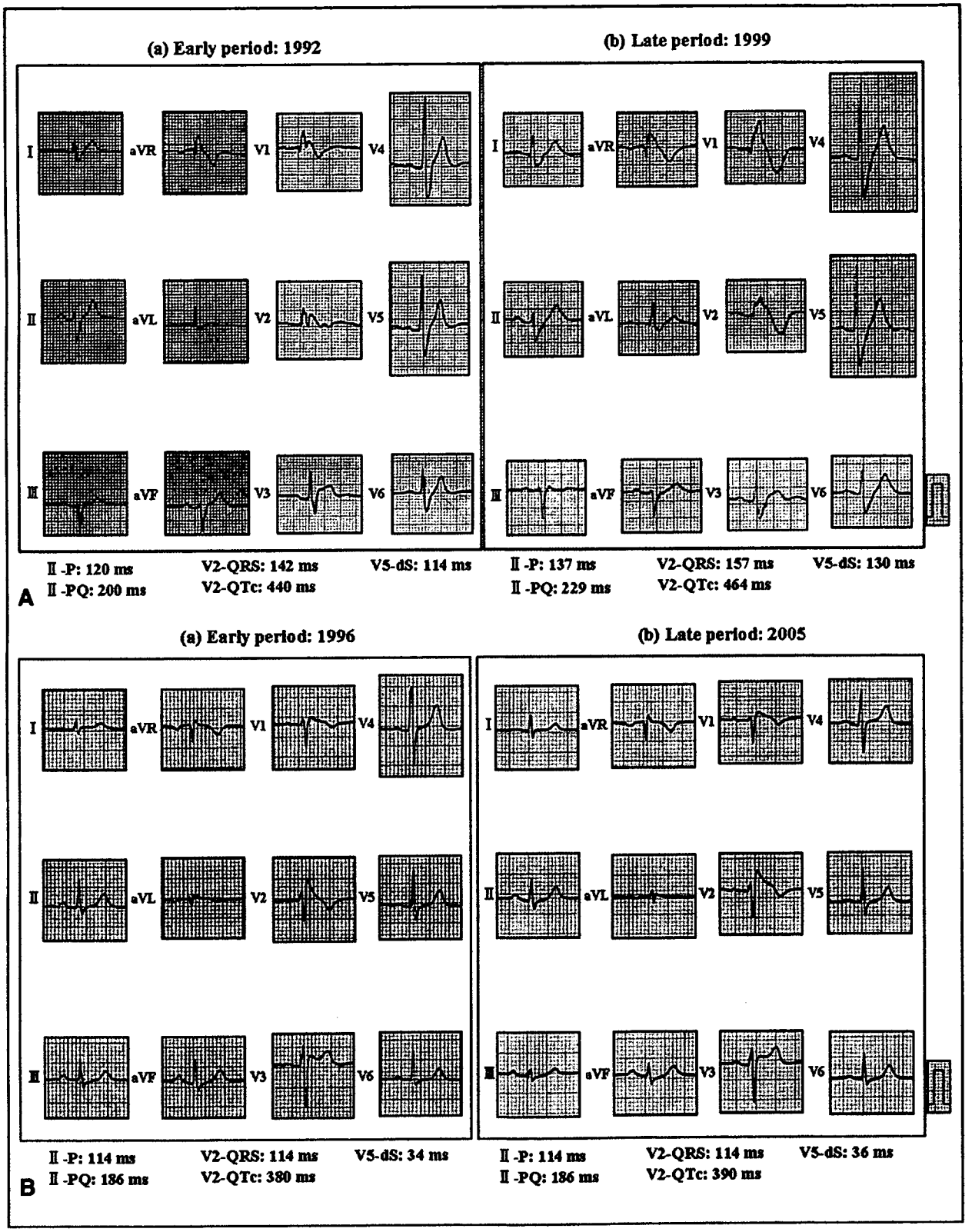

Figure 1. Standard 12-lead ECG at early and late periods during follow-up in representative cases of BS. *A*, in an *SCN5A*-positive proband (follow-up period, 7 years), the P-wave (lead II), QRS (lead V_2), and S-wave (lead V_5) durations and PQ interval (lead II) were prolonged even at the early period (47 years of age, *a*). The S-wave amplitude (lead V_5) was also deep, and the QRS axis deviated to the left. The QTc interval (lead V_2) was borderline prolonged. At the late period (*b*), all these parameters further increased. *B*, in an SCN5A-negative proband (follow-up period, 9 years), the P-wave (lead II), QRS (lead V_2), and S-wave (lead V_5) durations, PQ interval (lead II), and QTc interval (lead V_2) were less prolonged compared with those in an SCN5A-positive proband at the early period (51 years of age, *a*). At the late period (*b*), these parameters did not change significantly. V_5-dS = S-wave duration in lead V_5.

Table 3
Electrocardiographic parameters during follow-up period

ECG Parameter (leads)	Early Period			Late Period		
	SCN5A-Positive Group (n = 8)	SCN5A-Negative Group (n = 36)	p Value	SCN5A-Positive Group (n = 8)	SCN5A-Negative Group (n = 36)	p Value
Heart rate (beats/min)	66 ± 11	64 ± 10	0.924	60 ± 6	67 ± 12	0.194
P-wave duration (II) (ms)	137 ± 21	110 ± 12	<0.001	155 ± 19†	119 ± 16†	<0.001
PQ interval (II) (ms)	227 ± 31	179 ± 18	<0.001	257 ± 22*	190 ± 22†	<0.001
QRS duration (II) (ms)	125 ± 22	102 ± 18	<0.001	142 ± 41‡	111 ± 19‡	<0.001
QRS duration (V_2) (ms)	135 ± 15	110 ± 13	<0.001	157 ± 28*	115 ± 16	<0.001
QRS duration (V_5) (ms)	130 ± 28	101 ± 15	<0.001	147 ± 42	108 ± 17	<0.001
S-wave duration (II) (ms)	65 ± 38	35 ± 24	<0.001	77 ± 54	43 ± 26‡	<0.001
S-wave duration (V_5) (ms)	69 ± 40	37 ± 19	<0.001	78 ± 50	49 ± 17*	<0.001
S-wave amplitude (II) (mV)	0.37 ± 0.23	0.23 ± 0.24	0.005	0.43 ± 0.24	0.21 ± 0.17	<0.001
S-wave amplitude (V_5) (mV)	0.83 ± 0.47	0.34 ± 0.25	<0.001	0.88 ± 0.48	0.47 ± 0.27†	<0.001
QRS axis (°)	44 ± 81	49 ± 43	0.954	10 ± 76‡	43 ± 41	0.001
QTc interval (II) (ms)	409 ± 37	396 ± 28	0.535	432 ± 40	410 ± 34	0.164
QTc interval (V_2) (ms)	427 ± 51	392 ± 37	0.038	471 ± 38‡	405 ± 38	<0.001
QTc interval (V_5) (ms)	401 ± 43	389 ± 29	0.593	408 ± 39	398 ± 36	0.746
JTc interval (II) (ms)	279 ± 32	290 ± 30	0.554	292 ± 44	293 ± 34	0.100
JTc interval (V_2) (ms)	285 ± 39	279 ± 35	0.960	316 ± 42	283 ± 38	0.044
JTc interval (V_5) (ms)	265 ± 26	286 ± 30	0.108	262 ± 42	283 ± 32	0.105
STJ amplitude (V_2) (mV)	0.42 ± 0.19	0.29 ± 0.13	0.014	0.37 ± 0.23	0.24 ± 0.17	0.011
STJ40 amplitude (V_2) (mV)	0.38 ± 0.14	0.23 ± 0.12	<0.001	0.34 ± 0.17	0.21 ± 0.15	0.006

Data are presented as means ± SD.
* $p < 0.001$ versus early period.
† $p < 0.01$ versus early period.
‡ $p < 0.05$ versus early period.
ECG = electrocardiographic; JTc = corrected JT; QTc = corrected QT; STJ amplitude = ST amplitude at J point; STJ 40 amplitude = ST amplitude 40 ms after J point.

Table 4
Comparison of the change of electrocardiographic parameters during follow-up

Change in ECG Parameter (leads)	SCN5A-Positive Group (n = 8)	SCN5A-Negative Group (n = 36)	p Value
Heart rate (beats/min)	−7 ± 10	3 ± 13	0.046
P-wave duration (II) (ms)	19 ± 12	9 ± 13	0.077
PQ interval (II) (ms)	30 ± 22	11 ± 14	0.004
QRS duration (II) (ms)	17 ± 22	8 ± 15	0.163
QRS duration (V_2) (ms)	22 ± 20	6 ± 11	0.003
QRS duration (V_5) (ms)	17 ± 29	8 ± 14	0.161
S-wave duration (II) (ms)	12 ± 17	8 ± 13	0.423
S-wave duration (V_5) (ms)	9 ± 15	12 ± 14	0.604
S-wave amplitude (II) (mV)	0.06 ± 0.10	−0.02 ± 0.14	0.152
S-wave amplitude (V_5) (mV)	0.05 ± 0.27	0.13 ± 0.18	0.331
QRS axis (°)	−34 ± 55	−6 ± 16	0.010
QTc interval (II) (ms)	22 ± 32	15 ± 34	0.562
QTc interval (V_2) (ms)	44 ± 49	13 ± 40	0.064
QTc interval (V_5) (ms)	6 ± 37	9 ± 30	0.845
JTc interval (II) (ms)	13 ± 27	3 ± 28	0.339
JTc interval (V_2) (ms)	31 ± 48	5 ± 38	0.094
JTc interval (V_5) (ms)	−3 ± 29	−3 ± 29	0.990
STJ amplitude (V_2) (mV)	−0.05 ± 0.18	−0.05 ± 0.12	0.949
STJ40 amplitude (V_2) (mV)	−0.04 ± 0.16	−0.02 ± 0.11	0.642

Abbreviations as in Table 3.

SCN5A mutation.[5,11] Smits et al[12] observed significantly longer PQ and HV intervals at baseline and a larger increase in PQ and QRS intervals after administration of sodium channel blockers in patients with BS with SCN5A mutations than in those without SCN5A mutations. Age-dependent variability in the conduction parameters was evidenced in SCN5A-positive patients with BS.[13,15] Moreover, this concept has been mechanistically investigated in vivo in heterozygous SCN5A mice, which showed progressive impairment with aging of atrial and

ventricular conduction associated with myocardial rearrangements and fibrosis.[16] Meregalli et al[17] showed prolongation of S-wave duration in leads II and III after administration of sodium channel blockers. Their group suggested that these electrocardiographic signs included reciprocal changes in the inferior leads, mirroring the conduction slowing in the RVOT,[17,18] which may progress with aging and relate to the pathogenesis of BS. In the present study, the P-wave, QRS, S-wave durations, and PQ intervals were all significantly longer, and the S-wave amplitude was significantly deeper in the SCN5A-positive group than in the SCN5A-negative group. In addition, the PQ interval and QRS duration in lead V_2 were more markedly prolonged, and the QRS axis deviated more to the left with aging in the SCN5A-positive group than in the SCN5A-negative group during the follow-up period. The results of previous clinical studies and the present study suggest that progressive depolarization abnormalities (i.e., conduction slowing) with aging may play a key role in the pathogenesis of BS.

It has been argued recently that arrhythmic events may occur when a sufficient degree of cell damage has been reached as a result of the severity of ion channel protein mutation. Frustaci et al[19] showed that myocyte apoptosis at the right and left ventricular myocardium was significantly higher in patients with BS with SCN5A mutations than in control subjects on histologic study. They suggested that abnormalities in the function of sodium channels may lead to cellular damage because intracellular sodium homeostasis has a relevant role in myocellular function.[19] Experimentally, Aiba et al[20] used a high-resolution optical mapping system in a pharmacologic BS model and demonstrated that depolarization abnormalities (i.e., conduction slowing) is required for the maintenance of VF in BS, although the initiating premature beats were a result of a phase 2 reentry mechanism. These histologic and experimental studies also support that progressive conduction abnormalities with aging may explain why an initial VF episode appears at middle to older ages, usually 40 to 50 years, in BS. It is generally accepted that SCN5A mutation is not associated with a higher risk of cardiac events, suggesting that genetic analysis is a useful diagnostic parameter but is not helpful for risk stratification.[7] Similarly, in the present study, the presence of SCN5A mutation did not predict subsequent arrhythmic events (Table 2). Most clinical studies have reported that induction of VF by programmed electrical stimulation did not predict the clinical outcome or clinical severity in patients with BS.[6,21,22] If the progressive conduction slowing with aging often observed in patients with BS, especially SCN5A-positve patients, are really linked to VF appearance, conduction parameters, such as QRS widening, late potentials, or inducibility of VF, may still have a potential to predict new or subsequent cardiac events.[23] A much larger patient population is required to make a definitive conclusion regarding the predictive value of SCN5A mutation and the conduction parameters for cardiac events.

Several clinical studies have suggested a localized QT prolongation, a repolarization parameter, in the right precordial leads (mainly lead V_2) in patients with BS.[24,25] Castro Hevia et al[25] have suggested that a QTc >460 ms in lead V_2 was a significant risk factor for subsequent cardiac events. We recently used 87-lead body surface ECGs and reported that a corrected recovery time, another repolarization parameter, was significantly longer in the right precordial body surface ECGs, reflecting the potentials of the RVOT, than in other body surface ECGs.[26] Similarly, in the present study, the longest QTc interval was observed in lead V_2 in most patients with BS with SCN5A mutation, who usually also had a coved-type ST-segment elevation and a terminal negative T wave. The fact that the QTc interval in lead V_2 was significantly longer in the SCN5A-positive patients than in the SCN5A-negative patients at the early and late periods can be explained by more frequent and higher coved-type ST-segment elevation with a terminal negative T wave in the SCN5A-positive patients. The QTc interval in lead V_2 was significantly prolonged from the early period to the late period in the SCN5A-positive patients; however, the JTc interval in lead V_2 did not change from the early period to the late period, suggesting that the significant QTc prolongation in lead V_2 with aging occurred mainly as a result of a significant prolongation of the QRS duration in lead V_2.

There are several limitations to the present study. First, because a small number of patients with BS with SCN5A mutation could be included in a single-center study, a larger number of patients with SCN5A mutation will be required to make a definitive conclusion. Second, the study population included 44 Brugada probands who could be prospectively followed up for average of 10 ± 5 years in our hospital. Therefore, the probands represent a severely affected population, but not a consecutively referred population. Third, Veltmann et al[27] recently reported the prevalence of fluctuations between diagnostic and nondiagnostic ECGs in patients with BS, which may influence the measurement of some electrocardiographic parameters, especially QT, JT interval, and ST amplitude, and should be taken into account. However, the influence of the fluctuations on depolarization parameters such as QRS duration is expected to be less pronounced.

1. Brugada P, Brugada J. Right bundle branch block, persistent ST segment elevation and sudden cardiac death: a distinct clinical and electrocardiographic syndrome: a multicenter report. *J Am Coll Cardiol* 1992;20:1391–1396.
2. Brugada J, Brugada P. Further characterization of the syndrome of right bundle branch block, ST segment elevation, and sudden cardiac death. *J Cardiovasc Electrophysiol* 1997;8:325–331.
3. Brugada J, Brugada R, Brugada P. Right bundle-branch block and ST-segment elevation in V1 through V3. A marker for sudden death in patients without demonstrable structural heart disease. *Circulation* 1998;97:457–460.
4. Wilde AA, Antzelevitch C, Borggrefe M, Brugada J, Brugada R, Brugada P, Corrado D, Hauer RN, Kass RS, Nademanee K, Priori SG, Towbin JA. Study Group on the Molecular Basis of Arrhythmias of the European Society of Cardiology. Proposed diagnostic criteria for the Brugada syndrome: consensus report. *Circulation* 2002;106:2514–2519.
5. Antzelevitch C, Brugada P, Borggrefe M, Brugada J, Brugada R, Corrado D, Gussak I, Lemarec H, Nademanee K, Perez Riera AR, et al. Brugada syndrome: report of the second consensus conference: endorsed by the Heart Rhythm Society and the European Heart Rhythm Association. *Circulation* 2005;111:659–670.
6. Priori SG, Napolitano C, Gasparini M, Pappone C, Della Bella P, Giordano U, Bloise R, Giustetto C, De Nardis R, Grillo M, Ronchetti E, Faggiano G, Nastoli J. Natural history of Brugada syndrome:

insights for risk stratification and management. *Circulation* 2002;105:1342–1347.
7. Priori SG, Napolitano C, Gasparini M, Pappone C, Della Bella P, Brignole M, Giordano U, Giovannini T, Menozzi C, Bloise R, et al. Clinical and genetic heterogeneity of right bundle branch block and ST-segment elevation syndrome: a prospective evaluation of 52 families. *Circulation* 2000;102:2509–2515.
8. Shimizu W, Aiba T, Kamakura S. Mechanisms of diseases: current understanding and future challenges in Brugada syndrome. *Nat Clin Pract Cardiovasc Med* 2005;2:408–414.
9. Nademanee K, Veerakul G, Nimmannit S, Chaowakul V, Bhuripanyo K, Likittanasombat K, Tunsanga K, Kuasirikul S, Malasit P, Tansupasawadikul S, Tatsanavivat P. Arrhythmogenic marker for the sudden unexplained death syndrome in Thai men. *Circulation* 1997;96:2595–2600.
10. Chen Q, Kirsch GE, Zhang D, Brugada R, Brugada J, Brugada P, Potenza D, Moya A, Borggrefe M, Breithardt G, et al. Genetic basis and molecular mechanism for idiopathic ventricular fibrillation. *Nature* 1998;392:293–296.
11. Alings M, Wilde A. "Brugada" syndrome: clinical data and suggested pathophysiological mechanism. *Circulation* 1999;99:666–673.
12. Smits JP, Eckardt L, Probst V, Bezzina CR, Schott JJ, Remme CA, Haverkamp W, Breithardt G, Escande D, Schulze-Bahr E, LeMarec H, Wilde AA. Genotype-phenotype relationship in Brugada syndrome: electrocardiographic features differentiate SCN5A-related patients from non- SCN5A-related patients. *J Am Coll Cardiol* 2002;40:350–356.
13. Probst V, Allouis M, Sacher F, Pattier S, Babuty D, Mabo P, Mansourati J, Victor J, Nguyen JM, Schott JJ, et al. Progressive cardiac conduction defect is the prevailing phenotype in carriers of a Brugada syndrome *SCN5A* mutation. *J Cardiovasc Electrophysiol* 2006;17:270–275.
14. Bezzina CR, Shimizu W, Yang P, Koopmann TT, Tanck MWT, Miyamoto Y, Kamakura S, Roden DM, Wilde AAM. A common sodium channel promoter haplotype in Asian subjects underlies variability in cardiac conduction. *Circulation* 2006;113:338–344.
15. Probst V, Kyndt F, Potet F, Trochu JN, Mialet G, Demolombe S, Schott JJ, Baro I, Escande D, Le Marec H. Haploinsufficiency in combination with aging causes *SCN5A*-linked hereditary Lenegre disease. *J Am Coll Cardiol* 2003;41:643–652.
16. Royer A, van Veen TA, Le Bouter S, Marionneau C, Griol-Charhbili V, Leoni AL, Steenman M, van Rijen HV, Demolombe S, Goddard CA, et al. Mouse model of SCN5A-linked hereditary Lenegre's disease: age-related conduction slowing and myocardial fibrosis. *Circulation* 2005;11:1738–1746.
17. Meregalli PG, Ruijter JM, Hofman N, Bezzina CR, Wilde AA, Tan HL. Diagnostic value or flecainide test in unmasking *SCN5A*-related Brugada syndrome. *J Cardiovasc Electrophysiol* 2006;17:857–864.
18. Tukkie R, Sogaard P, Vleugels J, de Groot IK, Wilde AA, Tan HL. Delay in right ventricular activation contributes to Brugada syndrome. *Circulation* 2004;109:1272–1277.
19. Frustaci A, Priori SG, Pieroni M, Chimenti C, Napolitano C, Rivolta I, Sanna T, Bellocci F, Russo MA. Cardiac histological substrate in patients with clinical phenotype of Brugada syndrome. *Circulation* 2005;112:3680–3687.
20. Aiba T, Shimizu W, Hidaka I, Uemura K, Noda T, Zheng C, Kamiya A, Inagaki M, Sugimachi M, Sunagawa K. Cellular basis for trigger and maintenance of ventricular fibrillation in the Brugada syndrome model: High resolution optical mapping study. *J Am Coll Cardiol* 2006;47:2074–2085.
21. Kanda M, Shimizu W, Matsuo K, Nagaya N, Taguchi A, Suyama K, Kurita T, Aihara N, Kamakura S. Electrophysiologic characteristics and implications of induced ventricular fibrillation in symptomatic patients with Brugada syndrome. *J Am Coll Cardiol* 2002;39:1799–1805.
22. Eckardt L, Probst V, Smits JP, Bahr ES, Wolpert C, Schimpf R, Wichter T, Boisseau P, Heinecke A, Breithardt G, et al. Long-term prognosis of individuals with right precordial ST-segment-elevation Brugada syndrome. *Circulation* 2005;111:257–263.
23. Shimizu W. Does an overlap syndrome really exist between Brugada syndrome and progressive cardiac conduction defect (Lenegre syndrome)? *J Cardiovasc Electrophysiol* 2006;17:276–278.
24. Pitzalis MV, Anaclerio M, Iacoviello M, Forleo C, Guida P, Troccoli R, Massari F, Mastropasqua F, Sorrentino S, Manghisi A, Rizzon P. QT-interval prolongation in right precordial leads: an additional electrocardiographic hallmark of Brugada syndrome. *J Am Coll Cardiol* 2003;42:1632–1637.
25. Castro Hevia J, Antzelevitch C, Tornes Barzaga F, Dorantes Sanchez M, Dorticos Balea F, Zayas Molina R, Quinones Perez MA, Fayad Rodriguez Y. Tpeak-Tend and Tpeak-Tend dispersion as risk factors for ventricular tachycardia/ventricular fibrillation in patients with the Brugada syndrome. *J Am Coll Cardiol* 2006;47:1828–1834.
26. Yokokawa M, Takaki H, Noda T, Satomi K, Suyama K, Kurita T, Kamakura S, Shimizu W. Spatial distribution of repolarization and depolarization abnormalities evaluated by body surface potential mapping in patients with Brugada syndrome. *Pacing Clin Electrophysiol* 2006;29:1112–1121.
27. Veltmann C, Schimpf R, Echternach C, Eckardt L, Kuschyk J, Streitner F, Spehl S, Borggrefe M, Wolpert C. A prospective study on spontaneous fluctuations between diagnostic and non-diagnostic ECGs in Brugada syndrome: implications for correct phenotyping and risk stratification. *Eur Heart J* 2006;27:2544–2552.

J Interv Card Electrophysiol (2007) 19:109–119
DOI 10.1007/s10840-007-9147-4

Implications of 2:1 atrioventricular block during typical atrioventricular nodal reentrant tachycardia

Kiyoshi Otomo · Kazuhiro Suyama · Hideo Okamura · Takashi Noda · Kazuhiro Satomi · Wataru Shimizu · Takashi Kurita · Naohiko Aihara · Shiro Kamakura

Received: 11 April 2007 / Accepted: 26 June 2007 / Published online: 1 August 2007

Abstract
Objective The effects of 2:1 AV block (AVB) on AV nodal reentrant tachycardia (AVNRT) remain to be elucidated. This study was performed to localize the site of 2:1 AVB and elucidate the effects of 2:1 AVB on typical AVNRT.
Methods The His bundle (HB) electrograms during typical AVNRT with 2:1 AV block were reviewed in 24 patients. It was hypothesized that if 2:1 AVB at the HB or below changed tachycardia cycle length (TCL), the lower turnaround point of the reentrant circuit (RC) might be located within the HB and parts of the HB might be involved in the RC.
Results A HB potential was absent in blocked beats during 2:1 AVB in four patients (supra-Hisian block), and the maximal amplitude of the HB potential in blocked beats was the same as that in conducted beats in four patients (infra-Hisian block), and was significantly smaller than that in conducted beats (0.1±0.1 versus 0.5±0.2 mV, $P<0.05$) in 16 patients (intra-Hisian block). Eight patients (33%) with intra-Hisian block had a nearly identical prolongation of the H–A and A–A intervals in blocked beats (12±3 and 13±2 ms, respectively) with unchanged A–H intervals, while the remaining 16 patients (67%) exhibited invariable A–A and/or H–A intervals.
Conclusion The site of 2:1 AVB during typical AVNRT was estimated to be at the HB or below in 83% of the cases. Two-to-one intra-Hisian block transiently prolonged TCL, possibly indicating involvement of the proximal HB in the RC in one-third of typical the AVNRT cases with 2:1 AVB.

Keywords Atrioventricular nodal reentrant tachycardia · Atrioventricular block · His bundle · Lower turnaround point

1 Introduction

Typical (slow–fast form) atrioventricular (AV) nodal reentrant tachycardia (AVNRT) occasionally exhibits 2:1 AV block without a tachycardia interruption, and which has been traditionally interpreted to suggest the presence of a lower common pathway between the reentrant circuit and His bundle [1, 2]. More recently, 2:1 AV block during typical AVNRT was reportedly due to a functional conduction block within or below the His bundle in the majority of the patients [3, 4]. Several studies presented the possibility that the lower turnaround point of the reentrant circuit in typical AVNRT was located at the proximal His bundle and the proximal part of the His bundle may be involved in the reentrant circuit [5–12]. Although 2:1 AV block during typical AVNRT has been conventionally believed to have no effect on the tachycardia itself [13], it may have some influence on the tachycardia timing intervals, assuming that the sites of the lower turnaround point as well as the sites of the 2:1 AV block are located close to one another within the proximal His bundle (Fig. 1).

The purposes of this study were to (1) localize the site of the 2:1 AV block during typical AVNRT, (2) assess the effects of the 2:1 AV block during typical AVNRT on the tachycardia timing intervals, and (3) localize the lower

K. Otomo · K. Suyama · H. Okamura · T. Noda · K. Satomi · W. Shimizu · T. Kurita · N. Aihara · S. Kamakura
Division of Cardiology, National Cardiovascular Center, Suita, Japan

K. Otomo (✉)
Division of Cardiology, Cardiovascular Center, Tsuchiura Kyodo Hospital, 11-7 Manabe-shin-machi, Tsuchiura, Ibaraki Prefecture 300-0053, Japan
e-mail: k-otomo@tj8.so-net.ne.jp

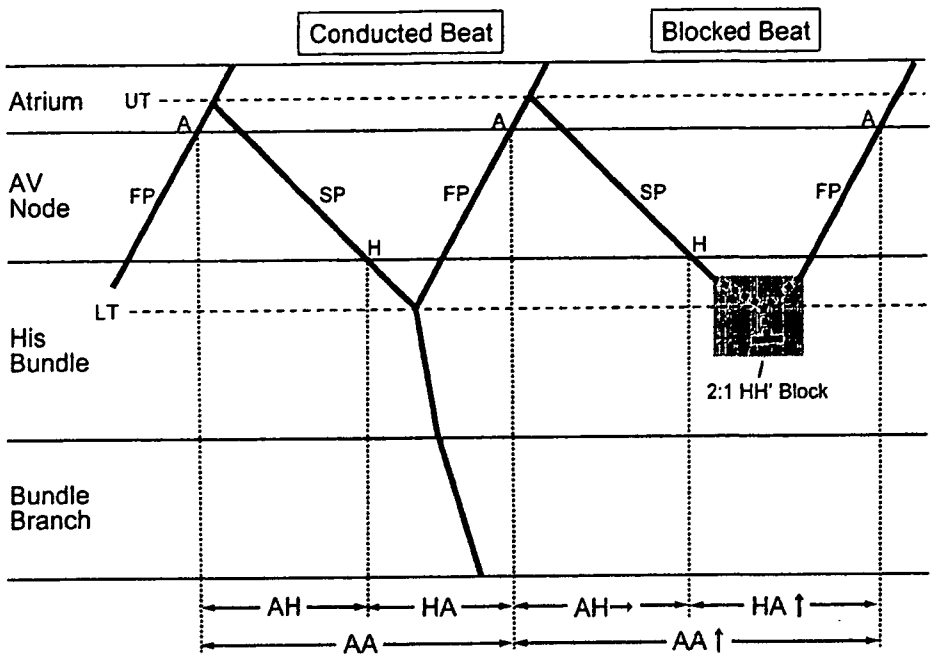

Fig. 1 The hypothetical reentrant circuit depicted by the laddergram showing the activation sequence during a typical AVNRT with 2:1 HH' block and the hypothetical mechanism by which the 2:1 HH' block influences the tachycardia timing intervals. The *shaded area* indicates the area with a functional conduction delay and block during 2:1 AV block. See the text for details. *A* represents the earliest atrial electrogram; *FP* retrograde fast pathway; *H* the earliest His bundle potential; *LTP* lower turnaround point; *SP* anterograde slow pathway; and *UTP* upper turnaround point

turnaround point of the reentrant circuit to assess if parts of the His bundle were involved in the reentrant circuit of the typical AVNRT.

2 Methods

2.1 Patients

This study included 24 consecutive patients who had at least one episode of typical AVNRT with sustained 2:1 AV block that lasted for more than 30 seconds during the electrophysiological study. These 24 patients accounted for 8% out of the 302 patients who had inducible typical AVNRT during the electrophysiological study in our institution. There were 10 men and 14 women with a mean age of 47±15 years. The mean sinus cycle length (CL), atrio-His (AH) interval and His-ventricular (HV) interval during sinus rhythm were 909±102, 78±18 and 40±5 ms, respectively. Two patients (8%) had right bundle branch block during sinus rhythm.

2.2 Electrophysiological study

The study protocol was reviewed and approved by the Institutional Committee on Human Research at the National Cardiovascular Center and each patient gave written informed consent prior to the procedure. All antiarrhythmic drugs had been discontinued for at least five half-lives before the procedures. With the patients under local anesthesia, venous access was obtained from the femoral and antecubital veins to introduce 4 electrode catheters. Three multipolar catheters were introduced from the femoral veins and positioned in the high right atrium, His bundle region and right ventricular apex. A His bundle catheter (decapolar catheter with a 1 mm-electrode width and 2-mm-inter-electrode spacing) was positioned across the tricuspid annulus so as to record the most proximal His bundle potential. An octapolar catheter was introduced from the right antecubital vein and positioned within the coronary sinus. Baseline electrophysiological evaluations and tachycardia inductions were performed during incremental pacing and extrastimulation (basic CL: 500–700 ms) from the right ventricular apex, high right atrium and coronary sinus using a programmable cardiac stimulator (EP-3 Computerized Stimulator, EP Med Systems, Inc., West Berlin, NJ, USA) with a pulse width of 2 ms and stimulus output of twice the diastolic pacing threshold. If AVNRT was not induced at baseline, isoproterenol (0.5–2.0 mg/min) was administered intravenously to facilitate the tachycardia induction. The intracardiac bipolar electrocardiograms were filtered through a bandpass of 30–500 Hz, displayed on a real-time monitor at a paper speed of 100 mm/s and stored with a 2-kHz sampling frequency on magneto-optical disks (Bard LabSystem Duo, Bard Electrophysiology, Lowell, MA, USA; or CardioLab, Prucka Engineering, Inc., Houston, TX, USA).

The exclusion of the tachycardia mechanisms other than AVNRT and diagnosis of AVNRT were performed based upon the classical criteria [13]. The absence of an AV accessory pathway was confirmed by the following criteria: ventricular pre-excitation was absent during sinus rhythm and atrial

pacing: the tachycardia was not reset by ventricular extrastimuli delivered during the most proximal His bundle's refractoriness; and para-Hisian pacing [14] during sinus rhythm exhibited a retrograde AV nodal conduction pattern. Atrial tachycardia and atrial flutter were excluded when a "V–A–V sequence" (not a "V–A–A–V sequence") was observed upon cessation of ventricular pacing associated with a 1:1 ventriculo-atrial conduction during the tachycardia [15]; the tachycardia was induced by ventricular pacing with a "V–A–V sequence"; and the tachycardia was reproducibly terminated with ventricular extrastimuli not reaching the atrium. The diagnosis of AVNRT was made if AV reciprocating tachycardia using AV accessory pathways and atrial tachycardia were excluded by the criteria mentioned above. The slow–fast form of AVNRT was diagnosed when the anterograde conduction occurred over the slow pathway with an AH interval during the tachycardia of 200 ms or longer; and the retrograde conduction proceeded over the fast pathway with the H–A interval during RV pacing at the tachycardia CL of less than 70 ms [16].

2.3 Definition and classification of the 2:1 AV block patterns during AVNRT

Sustained 2:1 AV block during typical AVNRT was defined as 2:1 AV block that persisted for 30 s or longer. The patterns of the 2:1 AV block were classified into one of the following: (1) AH block (supra-Hisian block), defined by the absence of any discernible His bundle potentials in the blocked beats, (2) HH' block (intra-Hisian block), defined by a lower amplitude (amplitude reduction of 50% or more) of the His bundle potentials in the blocked beats than those in the conducted beats, and (3) HV block (infra-Hisian block), defined by the same amplitudes of the His bundle potentials in the blocked and conducted beats.

2.4 Measurements of the electrophysiological parameters during AVNRT with 1:1 and 2:1 AV conduction

During the episodes of the typical AVNRT with sustained 2:1 AV block, the His bundle catheter was manipulated to maximize the amplitude of the His bundle potential in the conducted and blocked beats. From the recordings of the intracardiac electrocardiograms during the episodes of typical AVNRT with stable 2:1 AV block, the following parameters were retrospectively measured both in the conducted and blocked beats (Fig. 2): the atrial–atrial (AA) interval [AAC and AAB (in milliseconds), respectively]; His–atrial (HA) interval [HAC and HAB (in milliseconds), respectively]; AH interval [AHC and AHB (in milliseconds), respectively]; and amplitude of the His bundle potential as measured in the His bundle electrograms [HBC and HBB (in millivolts), respectively]. The increments of the AA interval [ΔAA (=AAB−AAC; in milliseconds)], HA interval [ΔHA (=HAB−HAC; in milliseconds)] and AH interval [ΔAH (=AHB−AHC; in milliseconds)] in the consecutive conducted and blocked beats were calculated. The percent reduction in the mean amplitude of the His bundle potential in the blocked beats as compared to that in the conducted beats [HBR (=100−

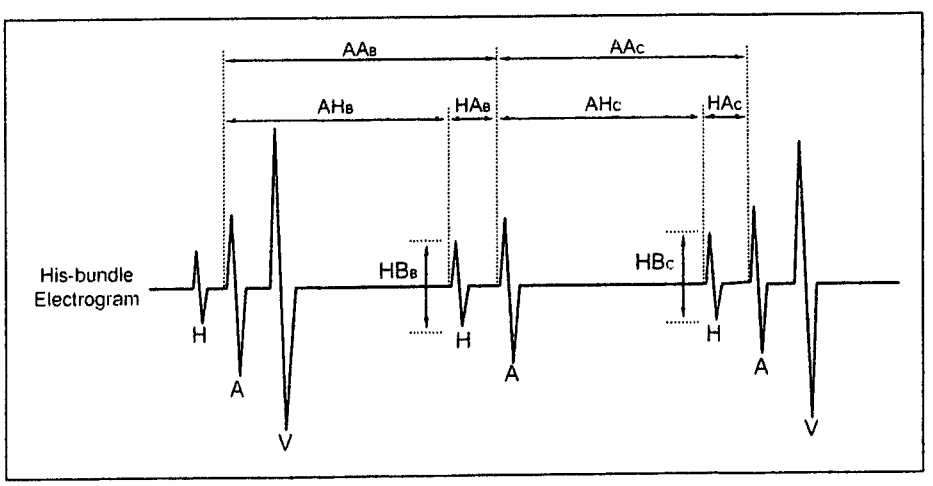

ΔAA (msec)=AAB−AAC
ΔAH (msec)=AHB−AHC
ΔHA (msec)=HAB−HAC
HBR (%)=100−HBB/HBC×100

Fig. 2 Schematic representation of the His bundle electrogram during typical AVNRT with 2:1 AV block, depicting the timing intervals measured in the present study. See the text for details

100×HBB/HBC; in percentage)] was calculated. The HAB, AHB, HBB, ΔHA, ΔAH and HBR were measured only in the patients with HH' and HV block. The AA, AH and HA intervals were also measured during episodes of typical AVNRT with 1:1 AV conduction just after conversion from 2:1 to 1:1 AV conduction. To exclude the influence of the basal instability of the tachycardia on the timing intervals, the electrocardiographic recordings within 30 s of the initiation and termination of the tachycardia were excluded from the analyses. Each parameter was measured for 20 consecutive beats with a paper speed of 100–200 mm/s and was presented as an average value. The 2:1 AV block during AVNRT was considered to have influenced the tachycardia if the ΔAA and/or ΔHA were 5 ms or longer.

2.5 Hypotheses

In this study, the site of the 2:1 AV block during the AVNRT was presumably determined according to the different AV block patterns during the episodes of 2:1 AV block [3, 4]. In the patients with 2:1 AH block during the AVNRT, the site of the block was assumed to be the lower common pathway within the AV node or junction between the AV node and His bundle. Among those with 2:1 HH' block, the site of the block was assumed to be the proximal part of the His bundle, because the block within the proximal His bundle would result in a reduction in the amount of the His bundle tissue depolarized and an amplitude reduction of the His bundle potential in the blocked beats [3, 4]. Among those with 2:1 HV block, the site of the block was assumed to be the distal His bundle or below.

In our hypothesis, 2:1 AV block at a site distant from the lower turnaround point of the reentrant circuit would be expected to have no effect on the AVNRT timing intervals. Assuming that 2:1 AV block occurred just below the lower turnaround point as a consequence of a transient conduction disturbance around the lower turnaround point, it would be expected to change the timing intervals of the AVNRT (Fig. 1). Therefore, it was hypothesized that if 2:1 AV block at the His bundle or below prolonged the AA and/or HA intervals, the lower turnaround point would be located within the His bundle or below, and parts of the His bundle would be involved in the reentrant circuit of the typical AVNRT (Fig. 1).

2.6 Statistical analysis

All the continuous variables were expressed as the mean± standard deviation. The Wilcoxon *t* test and Mann–Whitney *U* test were used to compare the paired and unpaired variables, respectively. A *P* value of less than 0.05 was considered statistically significant.

3 Results

Among 24 patients with sustained 2:1 AV block during typical AVNRT, 4 (17%), 16 (66%) and 4 patients (17%) had AH, HH' and HV block, respectively (Figs. 3, 4 and 5). The mean AA interval was significantly shorter during the 2:1 than 1:1 AV conduction (300±23 versus 308±23 ms; $P<0.01$). The 2:1 AV block occurred just after the initiation of AVNRT in 14 (58%), spontaneously with the shortening of the AA interval under the infusion of isoproterenol in 6 (25%), or after spontaneous or induced ventricular premature depolarizations in 4 patients (17%). The episodes of

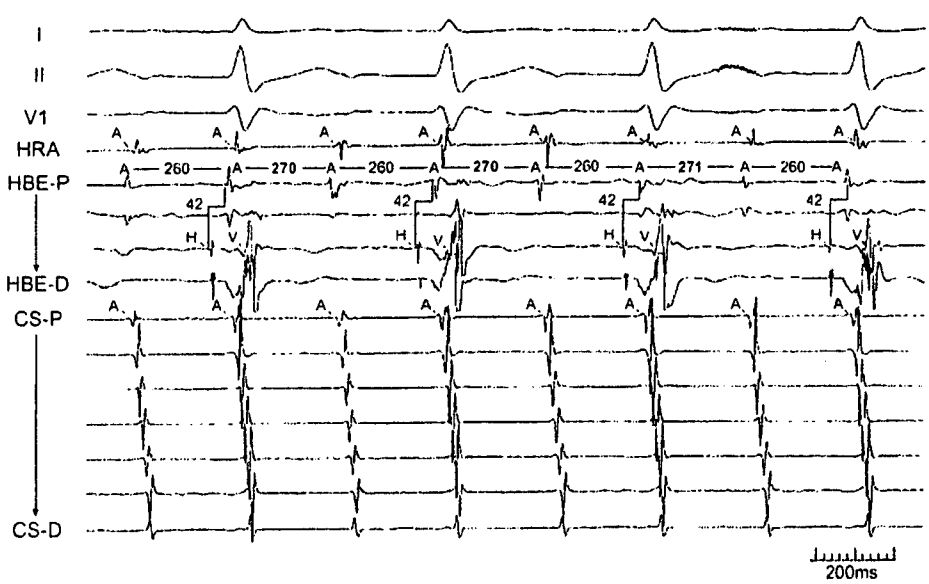

Fig. 3 Body-surface and intracardiac electrocardiograms during 2:1 AH block. Small but distinct prolongations were observed in the AAB. All figures are in millisecond. See the text for details. *CS-D* and *CS-P* represent the distal and proximal bipole pairs of the coronary sinus catheter, respectively; *HBE-D* and *HBE-P*, distal and proximal bipole pairs of the His bundle catheter, respectively; and HRA, high right atrium

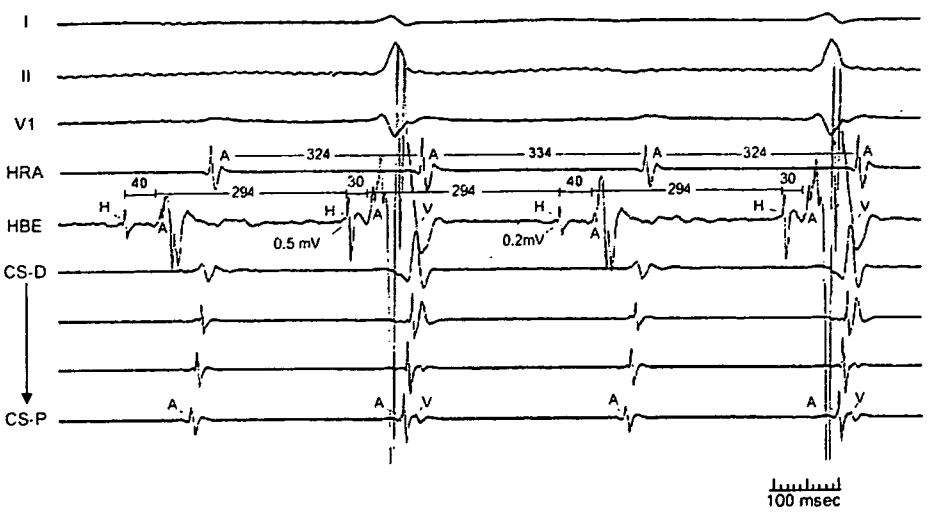

Fig. 4 Body-surface and intracardiac electrocardiograms during 2:1 HH' block. Nearly identical prolongations were observed in the AAB and HAB with an invariable AHB. All figures are in millisecond unless otherwise indicated. See the text for details. The abbreviations are as in the previous figures

the AVNRT with sustained 2:1 AV block occurred once in 7 (29%), twice in 7 (29%), three times in 9 (38%) and four times in 1 patient (4%). The conversion from 2:1 to 1:1 AV conduction was observed in all 24 patients (100%), and occurred in association with a spontaneous prolongation in the AA and AH intervals in 24 patients (100%) and/or after the introduction of a single ventricular extrastimulus in 4 patients (17%).

3.1 Influence of the 2:1 AV block on the AVNRT with the different AV block patterns

The influence of the 2:1 AV block on the typical AVNRT in the different AV block patterns is summarized in Table 1. Among the four patients with AH block, three patients (75%) exhibited a prolongation of the AAB as compared to the AAC during the AVNRT with 2:1 AV block (AAC: 298±33 ms, AAB: 309±34 ms: $P>0.05$, ΔAA: 11±1 ms; Fig. 3), which disappeared as soon as the 1:1 AV conduction resumed (AA, AH, and HA intervals during the tachycardia with 1:1 AV conduction: 303±52, 255±18, and 48±7 ms, respectively). In one other patient (25%) with AH block, the AAB and AAC were similar during the AVNRT with 2:1 AV block (AAC: 310 ms, AAB: 312 ms, ΔAA: 2 ms). Among the 16 patients with HH' block, 8 patients (50%) exhibited nearly identical prolongations in the AAB and HAB as compared to the AAC and HAC, respectively (AAC: 298±25 ms, AAB: 310±24 ms: $P<0.05$,

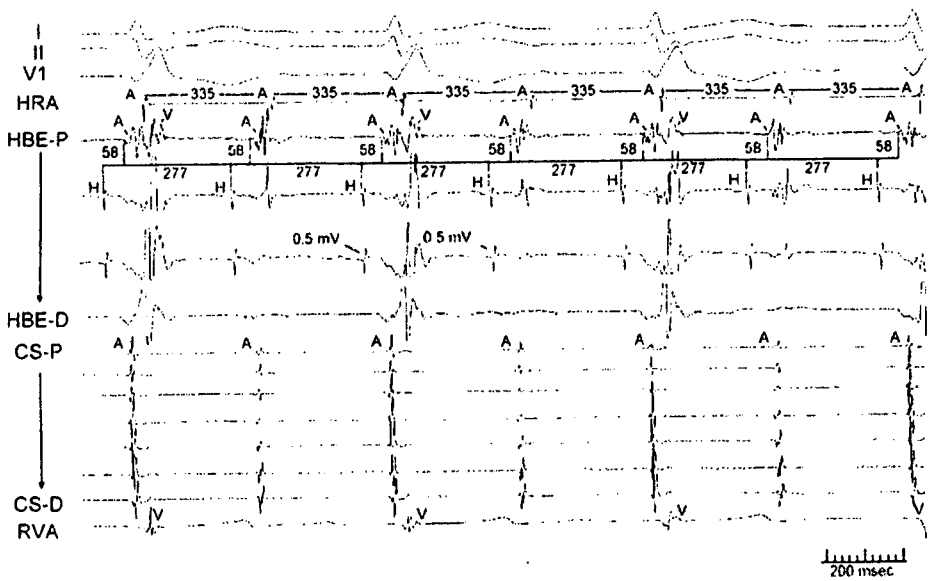

Fig. 5 Body-surface and intracardiac electrocardiograms during 2:1 HV block. No prolongation was observed in the AAB and HAB. All figures are in millisecond unless otherwise indicated. See the text for details. *RVA* represents the right ventricular apex. The other abbreviations are as in the previous figures

Table 1 Influence of 2:1 AV block on the slow-fast AVNRT in different AV block patterns

Patterns of 2:1 AV block	AH block (n=4)		HH' block (n=16)		HV block (n=4)	
ΔAA, ΔHA	<5 ms (n=1)	≥5 ms (n=3)	<5 ms (n=8)	≥5 ms (n=8)	<5 ms (n=4)	≥5 ms (n=0)
ΔAA (ms)	2	11±1	0±2*	13±2*	0±2	-
ΔAH (ms)	-	-	1±1	0±1	1±1	-
ΔHA (ms)	-	-	−1±2*	12±3*	−1±1	-

*P< 0.01 by Mann–Whitney U test.

ΔAA: 13±2 ms, HAC: 49±13 ms, HAB: 62±14 ms; P< 0.05, ΔHA: 12±3 ms) with an invariable AHB (AHC: 249± 27 ms, AHB: 249±28 ms; P>0.05, ΔAH: 0±1 ms) during the AVNRT with 2:1 AV block (Fig. 4), which disappeared as soon as the 1:1 AV conduction resumed (Fig. 6). In the other 8 patients (50%) with HH' block, the AAB, AHB and HAB during 2:1 AV block were similar to the AAC, HAC and AHC, respectively (AAC: 300±20 ms, AAB: 300± 19 ms; P>0.05, ΔAA: 0±2 ms, AHC: 244±20 ms, AHB: 245±19 ms; P>0.05, ΔAH: 1±1 ms, HAC: 56±13 ms, HAB: 55±12 ms; P>0.05, ΔHA: −1±2 ms). Among the 16 patients with HH' block, the HBB was significantly smaller than HBC in both patient groups with and without prolongations in AAB and HAB (HBC and HBB in the 8 patients with prolongation in AAB and HAB: 0.5±0.2 versus 0.1±0.1 mV, respectively; P<0.05, HBC and HBB in the 8 patients without prolongation in AAB and HAB: HBC: 0.5±0.2 versus 0.1±0.1 mV, respectively; P<0.05). Among the 16 patients with HH' block, the HBR was not different between the patient groups with and without prolongations

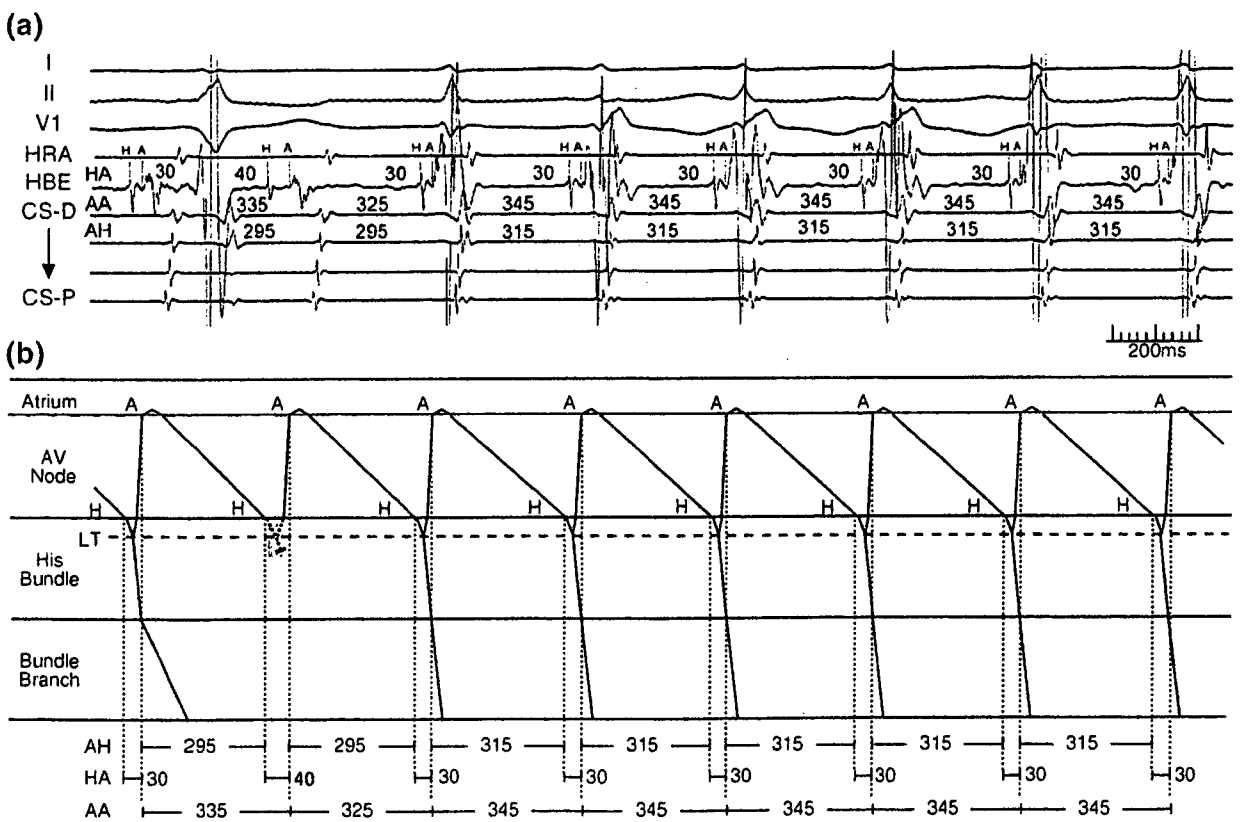

Fig. 6 Body-surface and intracardiac electrocardiograms (a) and the laddergram depicting the activation sequence during the conversion from 2:1 to 1:1 AV conduction in the same patient as in Fig. 4 (b). As soon as the 1:1 AV conduction resumed, the prolongations in HAB and AAB disappeared. The first QRS complex is associated with a transient complete left bundle branch block and a resultant HV interval prolongation. The *shaded area* indicates the area with a functional conduction delay and block during 2:1 AV block. All figures are in millisecond. See the text for details. The abbreviations are as in the previous figures

in AAB and HAB (81±7 versus 82±6%, respectively: $P>0.05$). None of the four patients with HV block exhibited prolongation in the AAB, AHB and HAB as compared to the AAC, AHC and HAC, respectively, during the AVNRT with 2:1 AV block (AAC: 290±27 ms, AAB: 290±28 ms: $P>0.05$, ΔAA: 0±2 ms, AHC: 245±51 ms, AHB: 246±51 ms: $P>0.05$, ΔAH: 1±1 ms, HAC: 45±24 ms, HAB: 44±23 ms: $P>0.05$, ΔHA: −1±1 ms: Fig. 5). Among the four patients with HH' block, there were no difference in the HBC and HBB (HBC: 0.5±0.3 mV, HBB: 0.5±0.2 mV: $P>0.05$, HBR: 3±6%).

Therefore, the 2:1 AV block during the typical AVNRT prolonged the HAB and/or AAB in 11/24 patients (46%). The nearly identical prolongations in the HAB (ΔHA: 12±3 ms) and AAB (ΔAA: 13±2 ms) in the eight patients (33%) with HH' block suggested the possibility that the lower turnaround point was located within the His bundle and 2:1 AV block occurred within the His bundle below the lower turnaround point.

3.2 Conversion from 2:1 to 1:1 AV conduction during typical atrioventricular nodal reentrant tachycardia

A spontaneous conversion from 2:1 to 1:1 AV conduction was observed in all 24 patients, and was associated with a slight prolongation in the AA interval in all episodes (mean AA intervals during 2:1 versus 1:1 AV conduction: 300±23 versus 308±23 ms, respectively; $P<0.01$), mainly due to the prolongation of the AH interval during the 1:1 AV conduction (mean AH intervals during 2:1 versus 1:1 AV conduction: 248±28 versus 257±23 milliseconds, respectively: $P<0.05$; Fig. 6). The AA, AH and HA intervals did not exhibit a beat-to-beat variation during the AVNRT with a stable 1:1 AV conduction in any of the 24 patients. The HA interval during the 1:1 AV conduction was similar to the HAC during the 2:1 AV block in all 24 patients (the HA interval during 1:1 AV conduction versus the HAC: 51±13 versus 50±14 ms, respectively: $P>0.05$), but was significantly shorter than the HAB in 8 patients with a prolongation in the AAB and HAB during the 2:1 HH' block (the HA interval during 1:1 AV conduction versus the HAB: 51±18 versus 62±14 ms, respectively: $P<0.05$). These findings supported the hypothesis that the 2:1 AV block during typical AVNRT was a consequence of a rate-dependent block around the lower turnaround point, and the prolongation in the HAB and AAB was derived from the conduction delay around the lower turnaround point associated with a 2:1 block just below the lower turnaround point.

3.3 Presumed sites of the 2:1 AV block and the lower turnaround

From the observations in this study, the site of the 2:1 AV block during the typical AVNRT was presumably localized to the distal part of the AV node or AV node–His bundle junction in 4 patients with AH block (17%), proximal part of the His bundle in 16 patients with HH' block (66%; Fig. 7), and distal His bundle or below it in 4 patients with HV block (17%). The lower turnaround point of the reentrant circuit was localized to the distal part of the AV node or AV node–His bundle junction in 4 patients with AH block (17%), and proximal part of the His bundle in

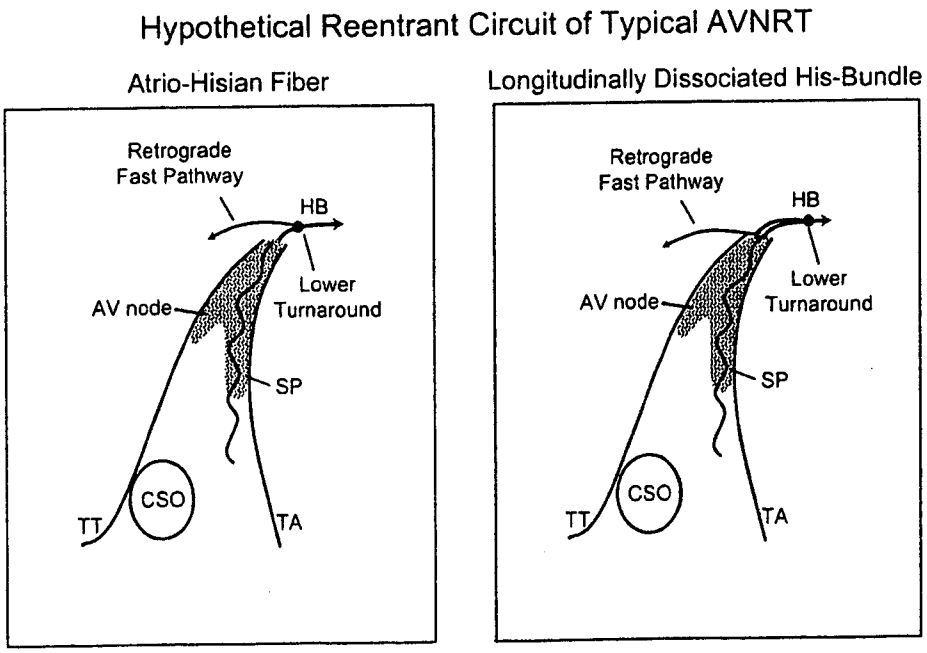

Fig. 7 Schematic representations of the hypothetical reentrant circuits of the typical AVNRT with the intra-Hisian location of the lower turnaround point. *Left*, reentrant circuit incorporating an atrio-Hisian fiber as the retrograde fast pathway. *Right*, reentrant circuit incorporating a longitudinally dissociated His bundle. See the text for details. *CSO* represents the ostium of the coronary sinus; *HB* His bundle; *SP* slow pathway; *TA* tricuspid annulus; and *TT* tendon of Todaro

8 patients with HH' block (33%). In 8 other patients with HH' block and 4 patients with HV block (50%), although the precise localization of the lower turnaround point was not feasible to determine from only the observations in this study, the lower turnaround point of the reentrant circuit was presumably localized to the AV node, AV node–His bundle junction, or proximal His bundle.

4 Discussion

4.1 Major findings

The present study showed that the site of the 2:1 AV block during the typical AVNRT was located in the His bundle or below in 83%, and the lower turnaround point of the reentrant circuit was located within the His bundle in at least 33% of the typical AVNRT cases exhibiting the 2:1 AV block during the tachycardia. Therefore, the proximal part of the His bundle might be involved in the reentrant circuit in at least one-third of the typical AVNRT cases exhibiting the 2:1 AV block.

4.2 Site of the 2:1 AV Block during typical atrioventricular nodal reentrant tachycardia

Previous reports [1–4, 17–20] have indicated that 2:1 AV block during AVNRT occurred either within the AV node, between the AV node and His bundle, within the His bundle or below. In the previous reports [1–4, 17–20] and this report, the localization of the exact site of the 2:1 AV block depended mainly on the evaluation of the His bundle potential in the blocked beats. However, Man et al. [3] reported that even without the His bundle potential in the blocked beats, the 2:1 AV block during typical AVNRT was due to functional infra-nodal block, because no conversion from 2:1 to 1:1 AV conduction was observed in response to the atropine administration. They concluded that most of the 2:1 AV block during typical AVNRT was due to functional infra-nodal block. In the present study, although not evaluated pharmacologically, the site of the 2:1 AV block was presumably localized to the His bundle or below it in 83% of the patients determined by evaluating the His bundle potential in the blocked beats, which was consistent with the results from the previous studies [3, 4].

4.3 Site of the lower turnaround point in typical atrioventricular nodal reentrant tachycardia

The site of the lower turnaround point of the reentrant circuit in typical AVNRT has been controversial [5–12, 21–25]. The present study showed that in at least 33% of typical AVNRT cases with 2:1 AV block, the lower turnaround point was located within the His bundle and the proximal part of the His bundle was involved in the reentrant circuit. Both the earlier [8–12] and recent studies [5–7, 21–23] also pointed out the possibility that the lower turnaround point of typical AVNRT was located within the His bundle and therefore the proximal part of the His bundle was involved in the reentrant circuit. The observations supporting the intra-Hisian location of the lower turnaround point included (1) the HA interval during ventricular pacing at the tachycardia rate was shorter than that during tachycardia [5–7]; (2) the presence of a retrograde fast pathway with a non-decremental property and resistance to adenosine, adenosine triphosphate or verapamil, suggested an atrio-Hisian fiber [5, 8–12, 26–29]; (3) the variation in the HA interval during typical AVNRT was simultaneous with the occurrence of HV block or bundle branch block [21, 22]; and (4) the tachycardia terminated with simultaneous HA and HV blocks [23]. Therefore, it is likely that in at least some patients, the lower turnaround point may be located within the His bundle, and the proximal part of the His bundle may be involved in the reentrant circuit of the typical AVNRT.

In the present study, the lower turnaround point was localized to the distal part of the AV node or AV node–His bundle junction in four patients with AH block (17%) and proximal part of the His bundle in eight patients with HH' block (33%), while in eight other patients with HH' block and four patients with HV block (50%), the precise localization of the lower turnaround point was not feasible to determine from only the observations in this study. In the latter 12 patients, the lower turnaround point of the reentrant circuit could be in the AV node, AV node–His bundle junction, or proximal His bundle. Those findings suggested that the lower turnaround point may be heterogeneously distributed around the AV node and proximal His bundle region in slow–fast AVNRT cases. In the 4 patients with HV block, 2:1 AV block did not have any influence on the tachycardia timing intervals; this finding could be interpreted to suggest that the lower turnaround point would not be located far distally at the distal His bundle or below in slow–fast AVNRT cases.

4.4 Effects of the 2:1 AV block during typical atrioventricular nodal reentrant tachycardia

As far as we know, only one study [20] has been reported in the literature evaluating the effects of 2:1 AV block on typical AVNRT. Lee et al. [20] reported that the AA_B was longer than the AAc in 21 (81%) of 26 patients with 2:1 AV block during AVNRT. In contrast to our results, they found that the prolongation in the AA_B was a consequence of the prolongation in the AH_B with an invariable HA_B, and they speculated that this phenomenon was caused by the

atrial stretch as a result of the ventricular contraction, or the phasic changes in the vagal tone caused by the blood pressure alternans during 2:1 AV conduction. Although no plausible explanation for these inconsistent results between the studies was available, the discrepancies might come from the relatively small sample sizes in both studies, different manners of measuring the timing intervals, or the relatively small changes in the AAB, AHB and HAB.

In the present study, the prolongations in the HAB and AAB observed in 11 patients (46%) indicated that 2:1 AV block occurred just below the lower turnaround point of the reentrant circuit and the transient conduction disturbance around the lower turnaround point gave rise to both 2:1 AV block below the lower turnaround point and a conduction delay at and/or just above the lower turnaround point. On the other hand, among 13 patients (54%) without any influence of the 2:1 AV block, the site of the 2:1 AV block was estimated to be located far distally from the lower turnaround point. Therefore, whether or not the 2:1 AV block during typical AVNRT influenced the AVNRT would probably be determined by the positional relationship between the lower turnaround point and the site of the 2:1 AV block.

4.5 Hypothetical models for the reentrant circuit with an Intra-Hisian location of the lower turnaround point

There could be at least two hypothetical explanations for the intra-Hisian location of the lower turnaround point (Fig. 7). The first one could be that the retrograde fast pathway consisted of a concealed atrio-Hisian fiber [30, 31] that originated from the proximal His bundle (Fig. 7, left) [5, 9–13, 32, 33]. The second one could be that there was a functional and longitudinal dissociation of the His bundle into two parts; one for the anterograde and the other for retrograde conduction during the tachycardia (Fig. 7, right) [22]. From the observations obtained from the present study, both hypotheses would be possible; however, the absence of double His bundle potentials during the tachycardia [34] would prefer the former explanation. The participation of a concealed atrio-Hisian fiber as a retrograde fast pathway has been reported in the literature [5, 9–13, 32, 33], and is compatible with the observations in this study.

4.6 Study limitations

This study had several limitations. The number of the patients included in the present study might be too small to convincingly prove our hypothesis. The determination of the exact site of the 2:1 AV block only by the evaluation of the His bundle potential in the blocked beats might be difficult. It might not be possible to record a very small His bundle potential from a conventional electrode catheter during 2:1 intra-Hisian block. Hence, even in those with no discernible His bundle potentials in the blocked beats during the 2:1 AV block, the intra Hisian block could not be definitively ruled out. Variations in the amplitudes of the recorded His bundle potentials during the 2:1 AV block might possibly be due to the catheter instability during the AVNRT with 2:1 AV block. The theoretical possibility that the His bundle potentials with a very low amplitude were generated from the distal AV node cannot be definitively ruled out. In the present study, a pharmacological assessment using drugs such as atropine was not performed to test if the 2:1 AV conduction converted to 1:1 AV conduction. The changes in the AAB and HAB during the 2:1 AV block were so small that only a margin of measurement error might have led to different results. The possibility that the prolongations in the AAB and HAB in only the blocked beats during the 2:1 AV block were derived from the beat-to-beat alternations in the conduction time over the retrograde fast pathway cannot be completely excluded. However, the invariable AH interval during the 2:1 AV block (AHc=AHB) with distinct prolongations in the AAB and HAB would argue against this possibility. Furthermore, the prolongation in the AAB and HAB during the 2:1 AV block completely disappeared as soon as the 1:1 AV conduction resumed after a subtle prolongation in the AA interval (Fig. 6), which suggested that the prolongations in the AAB and HAB were strongly related to the occurrence of the 2:1 AV block. The observation that the HA interval during the 1:1 AV conduction was similar to the HAc during the 2:1 AV block would also indicate that the prolongation in the HAB was strongly related to the 2:1 AV block. Nevertheless, the influence of the atrial stretch as a result of the ventricular contraction [35] and phasic changes in the vagal tone caused by the blood pressure alternans during the 2:1 AV conduction [36] on the changes in the timing intervals during the typical AVNRT with 2:1 AV block cannot be definitively excluded from the possible mechanisms.

5 Conclusion

The site of the 2:1 AV block during the tachycardia was located at the His bundle or below in 83% of the typical AVNRT cases with 2:1 AV block. The 2:1 AV block during the tachycardia prolonged the HA and/or AA intervals in the blocked beats in 11 patients (46%) of the typical AVNRT cases with 2:1 AV block. Similar prolongations in the HA and AA intervals in the blocked beats in eight patients (33%) with intra-Hisian block suggested that the lower turnaround point was located within the His bundle and the proximal part of the His bundle was involved in the reentrant circuit in at least one-third of the typical AVNRT cases with 2:1 AV block.